Paper 217

©Civil-Comp Press, 2012
Proceedings of the Eleventh International Conference
on Computational Structures Technology,
B.H.V. Topping, (Editor),
Civil-Comp Press, Stirlingshire, Scotland

Wave Spectral Finite Element Analysis of Two-Dimensional Waveguides

P.B. Silva and J.R.F. Arruda
Department of Computational Mechanics
Faculty of Mechanical Engineering
University of Campinas, SP, Brazil

Abstract

This paper shows that it is possible to build numerical spectral element matrices of two-dimensional waveguides using the dispersion parameters obtained from a thin slice of the waveguide modelled with conventional finite elements. The approach, called the wave spectral finite element method (WSFEM), was developed for applications in mid frequency analyses. In this paper, the mathematical formulation for a general structure is presented and particularized for a flat plate. The forced response of a thin plate simply-supported and free of constraints obtained by the WSFEM is compared with a finite element analyses in order to validate the proposed approach.

Keywords: waveguides, mid frequency, spectral element, finite element, higher-order modes, structural dynamics, propagation modes.

1 Introduction

There is a demand for reliable numerical models of wave propagation in long structures of arbitrary cross-section in the mid-frequency range. This is so, in part, to take advantage of the periodic characteristic of these structures, but it is also motivated by the advances in the oil industry that require increasingly longer risers. As analytical solutions do not exist for most of these structures and finite element simulation requires a prohibitive computational cost, hybrid methods have been proposed since the 1970's by Dong and Nelson [1], and later by Thompson [2] and Gavric [3]. This topic still attracts attention of many researchers, mainly interested in overcoming numerical problems that arise as frequency rises.

Two different methodologies have emerged from the earlier works of Dong and Nelson [1] and Mead [4]. The former one has motivated researchers to treat the displacement field of waveguides with one main axis and a constant cross section as a product of a spatial function that describes the wave motion of the cross-section plane and a complex exponential function to describe the wave propagation along the main axis. Therefore, only a 2-D mesh of the cross-section is required [5]. Nevertheless, this approach sometimes referred to semi-analytical finite element method (SAFE) [6-8], also known as waveguide finite elements [3] or spectral finite elements [9] must need the spectral stiffness matrices to be formulated on a case-by-case basis [10], which is not an insignificant task.

Based on the periodic structure theory developed by Mead [4], Thompson [3] has obtained the dispersion relations for a rail track by modelling a thin slice of the structure using conventional finite elements. Then, applying the periodic conditions and satisfying the continuity of displacement and the equilibrium at interface, an eigenvalue solution provides the wavenumbers and corresponding wave propagation modes. This procedure, usually known as wave and finite element method (WFEM), has been a decade later improved by Mace et al. [11]. Mencik [12] and Arruda et al. [13] have also proposed alternatives to circumvent numerical difficulties encountered when dealing with the problem. Using the wave parameters obtained from application of WFEM, different approaches have been derived to compute the forced response of a full structure. These approaches can be based on wave propagation solutions as proposed by Duhamel [10] or spectral element formulation as shown by Arruda and Nascimento [14].

This paper uses a straightforward approach based on a hybrid finite/spectral element method, also called Wave Spectral Finite Element Method (WSFEM). It consists in extracting wavenumbers and wave modes from a thin slice of the substructure modelled using conventional finite elements, and, subsequently, writing kinematic variables and internal forces in the spectral form using, respectively, the wave mode displacement and the wave mode force components.

In this work, the WSFEM is applied to a two-dimensional structure, namely a thin plate. The numerical forced responses are evaluated for low to mid-frequencies and are compared to full FE and spectral element analyses for validation.

In addition, as a way to avoid disparities between expected and predicted responses, the sources of numerical errors when solving the wave propagation problem are pointed out. The main sources of numerical errors are shown to be the eigenvalue problem, which must be solved to produce dispersion relations and the wave propagation modes, and the pseudo-inversion, used to obtain the spectral element matrix. As an alternative, the eigenvalue problem is solved using a companion equation proposed by Ahmida and Arruda [4], which prevents ill-conditioning of the original transfer matrix eigenvalue problem. This is an alternative to Zhong's formulation [5].

Besides the computational efficiency, the approach presented in this paper has the advantage of not requiring neither wave propagation solutions nor the use of elastodynamic equations. Furthermore, it has the potential to include the effect of higher order wave modes. This makes possible the study of complex cross-section shapes, particularly near boundaries or sharp edges [6]. The spectral finite element approach allows solving the problem using element-based direct stiffness method, which easily integrates wave spectral finite elements and ordinary finite elements and allows very arbitrary dynamic loading conditions. The effect of including a higher number of modes is discussed for a thin plate waveguide example.

2 Wave propagation analysis of periodic structures

Waveguides are structures that guide waves through one or more dimensions. This work particularly concerns those structures with one direction of symmetry, taken as the x-axis. The type of symmetry can vary; it can be a translational one, as, for example, an uniform rod, a plate strip with constant width, laminated composites, ducts or pipes, a rotational one, for instance, curved beams and tyres, or a periodic material arrangement.

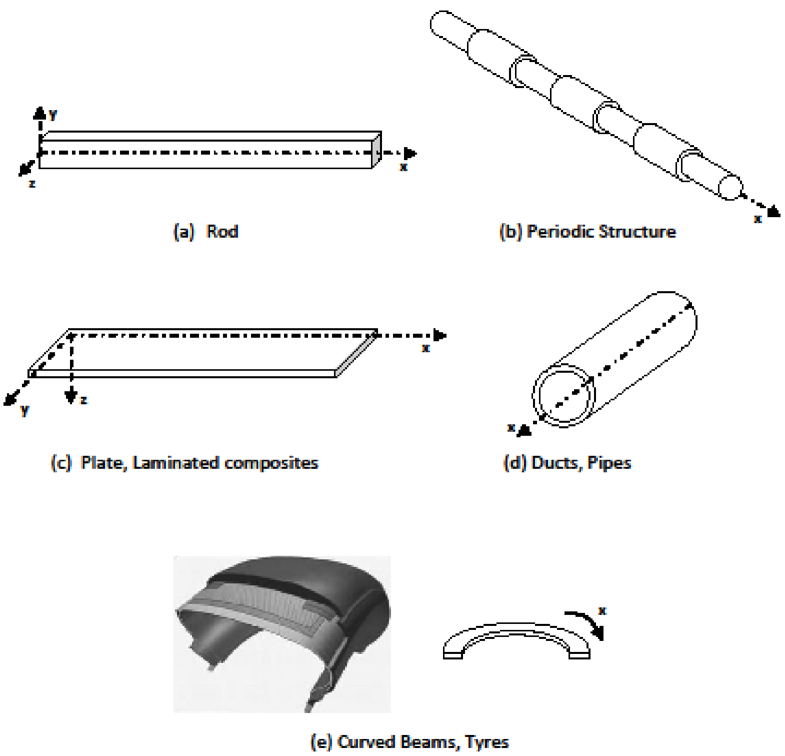

Figure 1: Examples of structures with one direction of symmetry (adapted from [10] and [11]).

2.1 Dynamic stiffness matrix of a waveguide slice

Symmetric waveguides can be considered as an arrangement of a finite or infinite number of cells. For wave propagation analysis purposes, a single cell of the structure with small thickness, Δ, usually smaller than $\lambda/6$ in order to avoid numerical discrepancies (spatial aliasing), is meshed with conventional finite elements (FE). In order to guarantee connectivity between substructures, left and right sides of the slice must be meshed with equal number and distribution of nodes, see Figure 2.

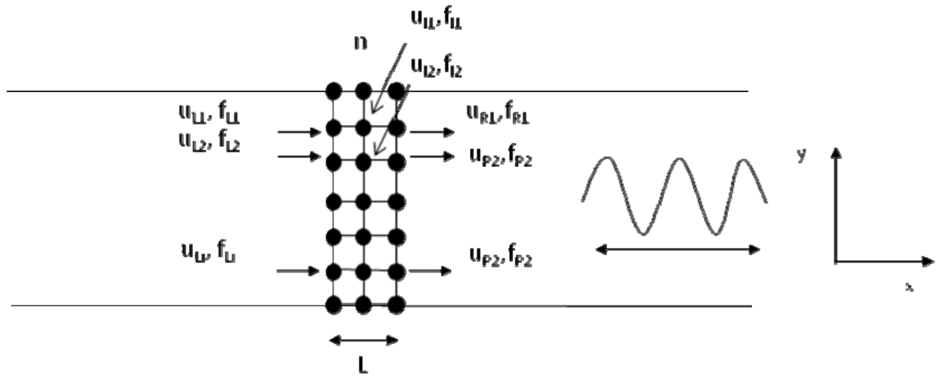

Figure 2: Representation of a waveguide section meshed with equal number of nodes on the left and right sides.

From the FE model, the mass, stiffness and damping matrices can be extracted and used to obtain the dynamic stiffness matrix for the slice at discrete frequencies. Thus, the equations of motion in the frequency domain for this substructure can be written as:

$$\mathbf{D}(\omega)\mathbf{q} = \mathbf{F} \tag{1}$$

where $\mathbf{D}(\omega) = \mathbf{K} + i\omega\mathbf{C} - \omega^2\mathbf{M}$ is the dynamic stiffness matrix, $\mathbf{K}$, $\mathbf{C}$ and $\mathbf{M}$ are the stiffness, damping and mass matrices, respectively, $\mathbf{q}$ is the displacement vector and $\mathbf{F}$, the applied force vector.

The terms of the dynamic stiffness matrix can be arranged in those related to the left degrees-of-freedom (DOFs), right and interior DOFs. Then, if no forces are applied at the interior nodes, the equations of motion can be written as:

$$\begin{bmatrix} \mathbf{D}_{LL} & \mathbf{D}_{LR} & \mathbf{D}_{LI} \\ \mathbf{D}_{RL} & \mathbf{D}_{RR} & \mathbf{D}_{RI} \\ \mathbf{D}_{IL} & \mathbf{D}_{IR} & \mathbf{D}_{II} \end{bmatrix} \begin{Bmatrix} \mathbf{q}_L \\ \mathbf{q}_R \\ \mathbf{q}_I \end{Bmatrix} = \begin{Bmatrix} \mathbf{F}_L \\ \mathbf{F}_R \\ \mathbf{0} \end{Bmatrix} \tag{2}$$

Using the third equation of the system of equations in Equation (2), the equations of motion can be written as function of the displacements at the left and right nodes only and a condensed dynamic stiffness matrix can be obtained, as expressed in Equation (3).

$$\begin{bmatrix} \hat{\mathbf{D}}_{LL} & \hat{\mathbf{D}}_{LR} \\ \hat{\mathbf{D}}_{RL} & \hat{\mathbf{D}}_{RR} \end{bmatrix} \begin{Bmatrix} \mathbf{q}_L \\ \mathbf{q}_R \end{Bmatrix} = \begin{Bmatrix} \mathbf{F}_L \\ \mathbf{F}_R \end{Bmatrix} \tag{3}$$

where $\hat{\mathbf{D}}_{LL} = \mathbf{D}_{LL} - \mathbf{D}_{LI}\mathbf{D}_{II}^{-1}\mathbf{D}_{IL}$, $\hat{\mathbf{D}}_{LR} = \mathbf{D}_{LR} - \mathbf{D}_{LI}\mathbf{D}_{II}^{-1}\mathbf{D}_{IR}$, $\hat{\mathbf{D}}_{RL} = \mathbf{D}_{RL} - \mathbf{D}_{RI}\mathbf{D}_{II}^{-1}\mathbf{D}_{IL}$ and

$\hat{\mathbf{D}}_{RR} = \mathbf{D}_{RR} - \mathbf{D}_{RI}\mathbf{D}_{II}^{-1}\mathbf{D}_{IR}$.

2.2 State-vector formulation

The dynamic system can be alternatively represented by a relation between the state vectors $\{\mathbf{q}_L ; \mathbf{f}_L\}$ and $\{\mathbf{q}_R ; \mathbf{f}_R\}$, where $\mathbf{f}_L$ and $\mathbf{f}_R$ are the internal forces at the left and right sides of the substructure, respectively. The general idea of this formulation is transform the partial differential equation that describes the dynamic system in a system of first-order ordinary differential equations whose solution is known. Thus, the transfer matrix is responsible for the relation between the state vector at the left side with the state vector at the right side of the slice, see Equation (4).

$$\mathbf{T}\begin{Bmatrix}\mathbf{q}_L \\ \mathbf{f}_L\end{Bmatrix} = \begin{Bmatrix}\mathbf{q}_R \\ \mathbf{f}_R\end{Bmatrix} \tag{4}$$

The internal and external forces are related by:

$$\mathbf{F}_L = -\mathbf{f}_L \tag{5.1}$$

$$\mathbf{F}_R = \mathbf{f}_R \tag{5.2}$$

Thus, the transfer matrix can be written by arranging the terms of the dynamic stiffness matrix:

$$[\mathbf{T}] = \begin{bmatrix} -\hat{\mathbf{D}}_{\mathbf{LR}}^{-1}\hat{\mathbf{D}}_{\mathbf{LL}} & -\hat{\mathbf{D}}_{\mathbf{LR}}^{-1} \\ \hat{\mathbf{D}}_{\mathbf{RL}} - \hat{\mathbf{D}}_{\mathbf{RR}}\hat{\mathbf{D}}_{\mathbf{LR}}^{-1}\hat{\mathbf{D}}_{\mathbf{LL}} & -\hat{\mathbf{D}}_{\mathbf{RR}}\hat{\mathbf{D}}_{\mathbf{LR}}^{-1} \end{bmatrix} \tag{6}$$

The continuity of displacements and the equilibrium at the interface between two substructures (k) and $(k+1)$ are satisfied by:

$$\mathbf{q}_R^{(k)} = \mathbf{q}_L^{(k+1)} \tag{7.1}$$

$$\mathbf{F}_R^{(k)} = -\mathbf{F}_L^{(k+1)} \tag{7.2}$$

Substituting Equations (7.1) and (7.2) in Equation (4) yields:

$$\mathbf{T}\begin{Bmatrix}\mathbf{q}_L^{(k)} \\ \mathbf{F}_L^{(k)}\end{Bmatrix} = \begin{Bmatrix}\mathbf{q}_L^{(k+1)} \\ -\mathbf{F}_L^{(k+1)}\end{Bmatrix} \tag{8}$$

The Bloch-Floquet theorem for periodic structures imposes a periodic condition to displacements and forces:

$$\mathbf{q}_L = \sum \overline{\mathbf{q}}_n(y,z)e^{-ik_n(\omega)x} \therefore \ \mathbf{q}_L^{(k+1)} = \lambda\,\mathbf{q}_L^{(k)} \tag{9.1}$$

$$\mathbf{f}_L = \sum \bar{\mathbf{f}}_n(y,z)e^{-ik_n(\omega)x} \;\therefore\; \mathbf{F}_L^{(k+1)} = -\lambda\, \mathbf{F}_L^{(k)} \tag{9.2}$$

Applying this theorem to Equation (8) yields the following eigenvalue problem:

$$\mathbf{T}\begin{Bmatrix}\mathbf{q}_L^{(k)}\\ \mathbf{F}_L^{(k)}\end{Bmatrix} = \lambda\begin{Bmatrix}\mathbf{q}_L^{(k)}\\ \mathbf{F}_L^{(k)}\end{Bmatrix} \tag{10}$$

Decomposing $\mathbf{T}$ in its eigenvalues and eigenvectors, the expression below is obtained:

$$\mathbf{T} = \mathbf{\Phi}\mathbf{\Lambda}\mathbf{\Phi}^{-1} \tag{11}$$

where $\mathbf{\Phi} = \left[\mathbf{\Phi}_q\,;\mathbf{\Phi}_F\right]$ and $\mathbf{\Lambda} = diag(\lambda_n) = diag(e^{-ik_n(\omega)\Delta})$.

From the eigenvalue decomposition, we conclude that the transfer matrix is the matrix exponential of the Hamiltonian matrix, which satisfies the symplectic inner product. Thus, from the Cayley-Hamilton theorem, the eigenvalues and eigenvectors of the transfer matrix satisfies the basic theorems of the symplectic space, which are defined below and have been demonstrated by Yao et al. [15].

Theorem 1: If μ is an eigenvalue of the Hamiltonian matrix with multiplicity *m*, then $-\mu$ is also an eigenvalue with multiplicity *m*.

Theorem 2: For $\mu_i + \mu_j \neq 0$, there is symplectic orthogonality between the corresponding normal eigenvectors, i.e., $\left\langle \mathbf{\Phi}_i, \mathbf{\Phi}_j \right\rangle = \mathbf{\Phi}_i^T \mathbf{J}\mathbf{\Phi}_j = 0$, where $[\mathbf{J}] = \begin{bmatrix} 0 & \mathbf{I}_N \\ -\mathbf{I}_N & 0\end{bmatrix}$.

Theorem 3: Let $\pm\mu \neq 0$ be a pair of mutually symplectic adjoint eigenvalues of the Hamiltonian matrix with multiplicity m, then there exists an adjoint symplectic orthonormal vector set

$$\left\{\mathbf{\Phi}_i^{(0)}, \mathbf{\Phi}_i^{(1)}, \ldots, \mathbf{\Phi}_i^{(m-1)}, \mathbf{\Phi}_j^{(m-1)}, \mathbf{\Phi}_j^{(m-2)}, \ldots, \mathbf{\Phi}_j^{(0)}\right\}$$

such that

$$\left\langle \mathbf{\Phi}_i^{(k)}, \mathbf{\Phi}_j^{(l)} \right\rangle = \begin{cases} (-1)^k a \neq 0 & when\ k+l = m-1 \\ 0 & when\ k+l \neq m-1 \end{cases}$$

As a consequence, the eigenvalues of Equation (10) occur in pairs λ_n and $1/\lambda_n$. Physically, the eigenvalues are related to the wavenumbers and the eigenvectors to the wave mode amplitudes expressed in coordinates of displacements and forces.

2.3 Alternative eigenvalue problem

The eigenvalue problem as stated in Equation (10) presents numerical ill-conditioning. These numerical problems are due in part to strong magnitude differences between transfer matrix terms, which are related to distinct dimensions of displacements and forces and, also, to the inversion of $\hat{D}_{LR}$, required to write the transfer matrix in terms of the dynamic stiffness matrix given from the FE model. In order to avoid numerical problems, in this work a companion eigenvalue problem is used, as proposed by Arruda and Ahmida [13].

Re-writing the system of equations defined in Equation (3) using the periodic condition established in Equation (7.1), gives:

$$\hat{\mathbf{D}}_{LL}\mathbf{q}_L + \hat{\mathbf{D}}_{LR}\mathbf{q}_R = \mathbf{F}_L \quad \therefore \quad \hat{\mathbf{D}}_{LL}\mathbf{q}_L + \hat{\mathbf{D}}_{LR}\lambda\mathbf{q}_L = \mathbf{F}_L \tag{12.1}$$

$$\hat{\mathbf{D}}_{RL}\mathbf{q}_L + \hat{\mathbf{D}}_{RR}\mathbf{q}_R = \mathbf{F}_R \quad \therefore \quad \hat{\mathbf{D}}_{RL}\mathbf{q}_L + \hat{\mathbf{D}}_{RR}\lambda\mathbf{q}_L = -\lambda\mathbf{F}_L \tag{12.2}$$

Now, substituting Equation (12.2) into (12.1) yields:

$$\hat{\mathbf{D}}_{RL}\mathbf{q}_L + \hat{\mathbf{D}}_{RR}\lambda\mathbf{q}_L = -\lambda\hat{\mathbf{D}}_{LL}\mathbf{q}_L + \lambda\hat{\mathbf{D}}_{LR}\lambda\mathbf{q}_L \quad \therefore \quad \lambda\left[(\hat{\mathbf{D}}_{LL} + \hat{\mathbf{D}}_{RR})\mathbf{q}_L - \hat{\mathbf{D}}_{LR}\lambda\mathbf{q}_L\right] = -\hat{\mathbf{D}}_{RL}\mathbf{q}_L \tag{13}$$

Thus, the associated eigenvalue problem is given by:

$$\begin{bmatrix} -\hat{\mathbf{D}}_{RL} & \mathbf{0} \\ \mathbf{0} & -\hat{\mathbf{D}}_{LR}^T \end{bmatrix} \begin{Bmatrix} \mathbf{q}_L \\ \lambda\mathbf{q}_L \end{Bmatrix} = \lambda \begin{bmatrix} \hat{\mathbf{D}}_{LL} + \hat{\mathbf{D}}_{RR} & -\hat{\mathbf{D}}_{LR} \\ -\hat{\mathbf{D}}_{LR}^T & \mathbf{0} \end{bmatrix} \begin{Bmatrix} \mathbf{q}_L \\ \lambda\mathbf{q}_L \end{Bmatrix} \tag{14}$$

Only the eigenvectors related to the displacement DOFs are directly obtained by solving the eigenvalue problem of Equation (14). The eigenvectors related to the force DOFs are obtained using the first equation in the system of equations in Equation (3).

$$\hat{\mathbf{D}}_{LL}\mathbf{\Phi}_{qn} + \hat{\mathbf{D}}_{LR}\lambda_n\mathbf{\Phi}_{qn} = \mathbf{\Phi}_{Fn} \quad \therefore \quad \hat{\mathbf{D}}_{LL}\mathbf{\Phi}_q + \hat{\mathbf{D}}_{LR}\mathbf{\Phi}_q\mathbf{\Lambda} = \mathbf{\Phi}_F \tag{15}$$

2.3.1 Frequency tracking of wave modes

The dispersion relations for the modelled structure can be obtained for discrete frequencies by solving the eigenvalue problem proposed in the previous section. Nevertheless, in order to plot the dispersion curves, the frequency tracking of the wave modes is an important task, as for each frequency the numerical eigenvalue solver usually sorts the wavenumbers by their magnitude. However, within a frequency range there are wavenumbers that cross over, and this is not accounted for in the ordinary sorting process.

There are at least two common procedures used for tracking wave modes: the modal assurance criteria (MAC) and a procedure based on the symplectic orthogonality between wave modes [12]. In this work, the latter procedure is adopted, as it seems to be more robust and it does not necessary need high frequency resolution as the MAC does.

Given two eigenvectors $\mathbf{\Phi}_j$ and $\mathbf{\Phi}_l$ evaluated at angular frequencies ω_{i-1} and ω_i, respectively, $k_j = -k_l$ if:

$$\left| \frac{\mathbf{\Phi}_j^H(\omega_{i-1})}{\left\|\mathbf{\Phi}_j(\omega_{i-1})\right\|} \mathbf{J} \frac{\mathbf{\Phi}_l(\omega_i)}{\left\|\mathbf{\Phi}_l(\omega_i)\right\|} \right| = \max_l \left\{ \frac{\mathbf{\Phi}_j^H(\omega_{i-1})}{\left\|\mathbf{\Phi}_j(\omega_{i-1})\right\|} \mathbf{J} \frac{\mathbf{\Phi}_l(\omega_i)}{\left\|\mathbf{\Phi}_l(\omega_i)\right\|} \right\} \tag{16}$$

It is important to note that, for a given mode, eigenvectors evaluated above the cut-on frequency are not symplectic orthogonal to those evaluated below this frequency [15].

3 Wave spectral finite element method

The WSFEM is based on the Spectral Element Method (SEM), as developed by Doyle [16], to write the displacement field. The SEM exactly describes the wave propagation dynamics within a structural element without discontinuities because the solution for the displacement field is written in the frequency domain (exact within the assumptions of the elastodynamic theory used in the formulation). Thus, as frequency rises, mesh refinement is not necessary. The WSFEM consists in obtaining the spectral matrix for an element of arbitrary length by using the wave parameters derived from the eigenvalue problem solved for a structure slice.

In the frequency domain, the general displacement for a structure can be written as:

$$\mathbf{q} = \sum_n \mathbf{A}e^{-ik_n x} + \mathbf{B}e^{ik_n x} = \sum_n A_n^+ \mathbf{\Phi}_{qn}^+ e^{-ik_n x} + A_n^- \mathbf{\Phi}_{qn}^- e^{ik_n x} \tag{17}$$

or, alternatively, as

$$\mathbf{q} = \sum_n \widetilde{A}_n^+ \mathbf{\Phi}_{qn}^+ e^{-ik_n x} + \widetilde{A}_n^- \mathbf{\Phi}_{qn}^- e^{ik_n (x-L)} \tag{18}$$

where $\widetilde{A}_n^+, \widetilde{A}_n^-$ are amplitude terms dependent on the boundary conditions. In matrix form, Equation (18) can be written as:

$$\mathbf{q} = \begin{bmatrix} \mathbf{\Phi}_q^+ [\mathbf{\Lambda}^+]^{\left(x/\Delta\right)} & \mathbf{\Phi}_q^- [\mathbf{\Lambda}^-]^{\left(x/\Delta\right)} [\mathbf{\Lambda}^+]^{\left(L/\Delta\right)} \end{bmatrix} \begin{Bmatrix} \widetilde{\mathbf{A}}^+ \\ \widetilde{\mathbf{A}}^- \end{Bmatrix} \tag{19}$$

For an element of length L, the displacements at the left and right sides are given by:

$$\begin{Bmatrix} \mathbf{q}_L \\ \mathbf{q}_R \end{Bmatrix} = \begin{bmatrix} [\mathbf{\Phi}_q^+].[\mathbf{I}] & [\mathbf{\Phi}_q^-].[\mathbf{\Lambda}^+]^{\left(L/\Delta\right)} \\ [\mathbf{\Phi}_q^+].[\mathbf{\Lambda}^+]^{\left(L/\Delta\right)} & [\mathbf{\Phi}_q^-].[\mathbf{I}] \end{bmatrix} \begin{Bmatrix} \tilde{\mathbf{A}}^+ \\ \tilde{\mathbf{A}}^- \end{Bmatrix} = [\mathbf{\Psi}]\{\tilde{\mathbf{A}}\} \tag{20}$$

Analogously, the forces can be written in the spectral form:

$$\mathbf{F} = \sum_n \mathbf{C}e^{-ik_n x} + \mathbf{D}e^{ik_n x} = \sum_n \tilde{A}_n^+ \mathbf{\Phi}_{Fn}^+ e^{-ik_n x} + \tilde{A}_n^- \mathbf{\Phi}_{Fn}^- e^{ik_n (x-L)} \tag{21}$$

In matrix form,

$$\mathbf{F} = \begin{bmatrix} \mathbf{\Phi}_F^+ [\mathbf{\Lambda}^+]^{\left(x/\Delta\right)} & \mathbf{\Phi}_F^- [\mathbf{\Lambda}^-]^{\left(x/\Delta\right)} [\mathbf{\Lambda}^+]^{\left(L/\Delta\right)} \end{bmatrix} \begin{Bmatrix} \tilde{\mathbf{A}}^+ \\ \tilde{\mathbf{A}}^- \end{Bmatrix} \tag{22}$$

At the left and right sides of an element of length L,

$$\begin{Bmatrix} \mathbf{F}_L \\ \mathbf{F}_R \end{Bmatrix} = \begin{bmatrix} -[\mathbf{\Phi}_F^+].[\mathbf{I}] & -[\mathbf{\Phi}_F^-].[\mathbf{\Lambda}^+]^{\left(L/\Delta\right)} \\ [\mathbf{\Phi}_F^+].[\mathbf{\Lambda}^+]^{\left(L/\Delta\right)} & [\mathbf{\Phi}_F^-].[\mathbf{I}] \end{bmatrix} \begin{Bmatrix} \tilde{\mathbf{A}}^+ \\ \tilde{\mathbf{A}}^- \end{Bmatrix} = [\overline{\mathbf{\Psi}}]\{\tilde{\mathbf{A}}\} \tag{23}$$

Manipulating Equation (20) in order to isolate the vector of amplitudes $\{\tilde{\mathbf{A}}\}$, gives:

$$\tilde{\mathbf{A}} = \left(\mathbf{\Psi}^H \mathbf{\Psi}\right)^{-1} \mathbf{\Psi}^H \begin{Bmatrix} \mathbf{q}_L \\ \mathbf{q}_R \end{Bmatrix} \tag{24}$$

Then, substituting Equation (24) into (23), yields:

$$\begin{Bmatrix} \mathbf{F}_L \\ \mathbf{F}_R \end{Bmatrix} = \overline{\mathbf{\Psi}} \left(\mathbf{\Psi}^H \mathbf{\Psi}\right)^{-1} \mathbf{\Psi}^H \begin{Bmatrix} \mathbf{q}_L \\ \mathbf{q}_R \end{Bmatrix} \tag{25}$$

Therefore, the numerical spectral matrix is given by:

$$\tilde{\mathbf{D}} = \overline{\mathbf{\Psi}} \left(\mathbf{\Psi}^H \mathbf{\Psi}\right)^{-1} \mathbf{\Psi}^H \tag{26}$$

The forced response of the structure is then easily obtained in a similar way harmonic responses are evaluated in FE analysis. Firstly, the global stiffness matrix is built by assembling the element matrices using the direct stiffness method. Then, applying the boundary conditions to this global numerical stiffness matrix, the displacement field is recovered simply by:

$$\mathbf{q} = \left[\tilde{\mathbf{D}}_G\right]_{BC}^{-1} \mathbf{F} \tag{27}$$

3.1 Wave spectral analysis of plates

A plate is a two-dimensional structure with one dimension significantly smaller than the other two. This modifies the behaviour of this structural element under wave propagation. Differently from the rod case, waves are not confined to follow a one-dimensional guide [16]. Nevertheless, in this work the two-dimensional problem will be reduced to a one-dimensional one by applying 1-D periodic conditions to a plate strip modelled with conventional FEs. This study, in the present form, is restricted to out-of-plane loads applied to thin plates. The response of the plate under different boundary conditions, sometimes a difficult task using analytical methods, is investigated. For instance, a spectral plate element is widely employed for a simply-supported plate in only one direction (two parallel sides simply supported). For other conditions, solutions are not possible or very cumbersome.

The displacement field of a thin plate under bending is described by the displacement in the *z*-direction, or transverse displacement, w, and rotations about the *x*- axis and the *y*-axis, θ_x and θ_y, respectively. The corresponding forces that can be applied to the structure are F_z, M_{xx} and M_{yy} . Thus, displacement and forces are written as:

$$\begin{Bmatrix} \mathbf{w} \\ \boldsymbol{\theta}_{\mathbf{x}} \\ \boldsymbol{\theta}_{\mathbf{y}} \end{Bmatrix} = \begin{bmatrix} \begin{bmatrix} \boldsymbol{\Phi}_{qz}^{+} \\ \boldsymbol{\Phi}_{\theta x}^{+} \\ \boldsymbol{\Phi}_{\theta y}^{+} \end{bmatrix} [\boldsymbol{\Lambda}^{+}]^{\left(x/\Delta\right)} & \begin{bmatrix} \boldsymbol{\Phi}_{qz}^{-} \\ \boldsymbol{\Phi}_{\theta x}^{-} \\ \boldsymbol{\Phi}_{\theta y}^{-} \end{bmatrix} [\boldsymbol{\Lambda}^{-}]^{\left(x/\Delta\right)} [\boldsymbol{\Lambda}^{+}]^{\left(L/\Delta\right)} \end{bmatrix} \begin{Bmatrix} \tilde{\mathbf{A}}^{+} \\ \tilde{\mathbf{A}}^{-} \end{Bmatrix} \tag{32}$$

$$\begin{Bmatrix} F_z \\ M_{\mathbf{xx}} \\ M_{\mathbf{yy}} \end{Bmatrix} = \begin{bmatrix} \begin{bmatrix} \boldsymbol{\Phi}_{Fz}^{+} \\ \boldsymbol{\Phi}_{F\theta x}^{+} \\ \boldsymbol{\Phi}_{F\theta y}^{+} \end{bmatrix} [\boldsymbol{\Lambda}^{+}]^{\left(x/\Delta\right)} & \begin{bmatrix} \boldsymbol{\Phi}_{Fz}^{-} \\ \boldsymbol{\Phi}_{F\theta x}^{-} \\ \boldsymbol{\Phi}_{F\theta y}^{-} \end{bmatrix} [\boldsymbol{\Lambda}^{-}]^{\left(x/\Delta\right)} [\boldsymbol{\Lambda}^{+}]^{\left(L/\Delta\right)} \end{bmatrix} \begin{Bmatrix} \tilde{\mathbf{A}}^{+} \\ \tilde{\mathbf{A}}^{-} \end{Bmatrix} \tag{33}$$

Manipulating Equation (32) and Equation (33), the displacements and forces at both sides of an element are given by:

$$\begin{Bmatrix} \mathbf{w}_L \\ \boldsymbol{\theta}_{\mathbf{x}L} \\ \boldsymbol{\theta}_{\mathbf{y}L} \\ \mathbf{w}_R \\ \boldsymbol{\theta}_{\mathbf{x}R} \\ \boldsymbol{\theta}_{\mathbf{y}R} \end{Bmatrix} = \begin{bmatrix} \begin{bmatrix} \boldsymbol{\Phi}_{qz}^{+} \\ \boldsymbol{\Phi}_{\theta x}^{+} \\ \boldsymbol{\Phi}_{\theta y}^{+} \end{bmatrix} . [\mathbf{I}] & \begin{bmatrix} \boldsymbol{\Phi}_{qz}^{-} \\ \boldsymbol{\Phi}_{\theta x}^{-} \\ \boldsymbol{\Phi}_{\theta y}^{-} \end{bmatrix} . [\boldsymbol{\Lambda}^{+}]^{\left(L/\Delta\right)} \\ \begin{bmatrix} \boldsymbol{\Phi}_{qz}^{+} \\ \boldsymbol{\Phi}_{\theta x}^{+} \\ \boldsymbol{\Phi}_{\theta y}^{+} \end{bmatrix} . [\boldsymbol{\Lambda}^{+}]^{\left(L/\Delta\right)} & \begin{bmatrix} \boldsymbol{\Phi}_{qz}^{-} \\ \boldsymbol{\Phi}_{\theta x}^{-} \\ \boldsymbol{\Phi}_{\theta y}^{-} \end{bmatrix} .. [\mathbf{I}] \end{bmatrix} \begin{Bmatrix} \tilde{\mathbf{A}}^{+} \\ \tilde{\mathbf{A}}^{-} \end{Bmatrix} = [\boldsymbol{\Psi}]\{\tilde{\mathbf{A}}\} \tag{34}$$

$$\begin{Bmatrix} F_{zL} \\ M_{\mathbf{xx}L} \\ M_{\mathbf{yy}L} \\ F_{zR} \\ M_{\mathbf{xx}R} \\ M_{\mathbf{yy}R} \end{Bmatrix} = \begin{bmatrix} -\begin{bmatrix} \mathbf{\Phi}_{Fz}^{+} \\ \mathbf{\Phi}_{F\theta x}^{+} \\ \mathbf{\Phi}_{F\theta y}^{+} \end{bmatrix} \cdot [\mathbf{I}] & -\begin{bmatrix} \mathbf{\Phi}_{Fz}^{-} \\ \mathbf{\Phi}_{F\theta x}^{-} \\ \mathbf{\Phi}_{F\theta y}^{-} \end{bmatrix} \cdot [\mathbf{\Lambda}^{+}]^{\left(L/\Delta\right)} \\ \begin{bmatrix} \mathbf{\Phi}_{Fz}^{+} \\ \mathbf{\Phi}_{F\theta x}^{+} \\ \mathbf{\Phi}_{F\theta y}^{+} \end{bmatrix} \cdot [\mathbf{\Lambda}^{+}]^{\left(L/\Delta\right)} & \begin{bmatrix} \mathbf{\Phi}_{Fz}^{-} \\ \mathbf{\Phi}_{F\theta x}^{-} \\ \mathbf{\Phi}_{F\theta y}^{-} \end{bmatrix} \cdot [\mathbf{I}] \end{bmatrix} \begin{Bmatrix} \tilde{\mathbf{A}}^{+} \\ \tilde{\mathbf{A}}^{-} \end{Bmatrix} = [\mathbf{\Psi}]\{\tilde{\mathbf{A}}\} \tag{35}$$

The numerical dynamic stiffness matrix is, thus, written as:

$$[\tilde{\mathbf{D}}] = \begin{bmatrix} -\begin{bmatrix} \mathbf{\Phi}_{Fz}^{+} \\ \mathbf{\Phi}_{F\theta x}^{+} \\ \mathbf{\Phi}_{F\theta y}^{+} \end{bmatrix} \cdot [\mathbf{I}] & -\begin{bmatrix} \mathbf{\Phi}_{Fz}^{-} \\ \mathbf{\Phi}_{F\theta x}^{-} \\ \mathbf{\Phi}_{F\theta y}^{-} \end{bmatrix} \cdot [\mathbf{\Lambda}^{+}]^{\left(L/\Delta\right)} \\ \begin{bmatrix} \mathbf{\Phi}_{Fz}^{+} \\ \mathbf{\Phi}_{F\theta x}^{+} \\ \mathbf{\Phi}_{F\theta y}^{+} \end{bmatrix} \cdot [\mathbf{\Lambda}^{+}]^{\left(L/\Delta\right)} & \begin{bmatrix} \mathbf{\Phi}_{Fz}^{-} \\ \mathbf{\Phi}_{F\theta x}^{-} \\ \mathbf{\Phi}_{F\theta y}^{-} \end{bmatrix} \cdot [\mathbf{I}] \end{bmatrix} \cdot \begin{bmatrix} \begin{bmatrix} \mathbf{\Phi}_{qz}^{+} \\ \mathbf{\Phi}_{\theta x}^{+} \\ \mathbf{\Phi}_{\theta y}^{+} \end{bmatrix} \cdot [\mathbf{I}] & \begin{bmatrix} \mathbf{\Phi}_{qz}^{-} \\ \mathbf{\Phi}_{\theta x}^{-} \\ \mathbf{\Phi}_{\theta y}^{-} \end{bmatrix} \cdot [\mathbf{\Lambda}^{+}]^{\left(L/\Delta\right)} \\ \begin{bmatrix} \mathbf{\Phi}_{qz}^{+} \\ \mathbf{\Phi}_{\theta x}^{+} \\ \mathbf{\Phi}_{\theta y}^{+} \end{bmatrix} \cdot [\mathbf{\Lambda}^{+}]^{\left(L/\Delta\right)} & \begin{bmatrix} \mathbf{\Phi}_{qz}^{-} \\ \mathbf{\Phi}_{\theta x}^{-} \\ \mathbf{\Phi}_{\theta y}^{-} \end{bmatrix} \cdot\cdot [\mathbf{I}] \end{bmatrix}^{+} \tag{36}$$

where the symbol + signifies that the pseudo-inversion is required.

4 Forced Response of a homogeneous plate from a 2D FEM model

Initially, the forced response of a homogeneous plate simply-supported along its edges by WSFEM is shown to agree well with results from SEM and conventional FEM. After, a free plate subjected to a harmonic excitation is analysed by WSFEM and the results compared to FE simulations.

4.1 Analysis of simply-supported plate along all edges

As discussed in section 3.2, a plate strip is modelled with SHELL63 finite elements, from the commercial software ANSYS®, with bending capability only. Based on previous work of Waki [17], it's known that dispersion relations are correctly extracted from a FE model of plate if the element size in x and y directions are approximately equal. For a first analysis, a steel plate ($\rho = 7800\,Kg/m^3,\ \ E = 210\,GPa,\ \ \nu = 0.3$) with $L_x = 1/30\,m$, $L_y = 1\,m$, $h = 0.001\,m$, $N_x = 2$ and $N_y = 60$, where N is the number of finite elements in a given direction, is modelled with FEs. Figure 3 shows this plate strip meshed.

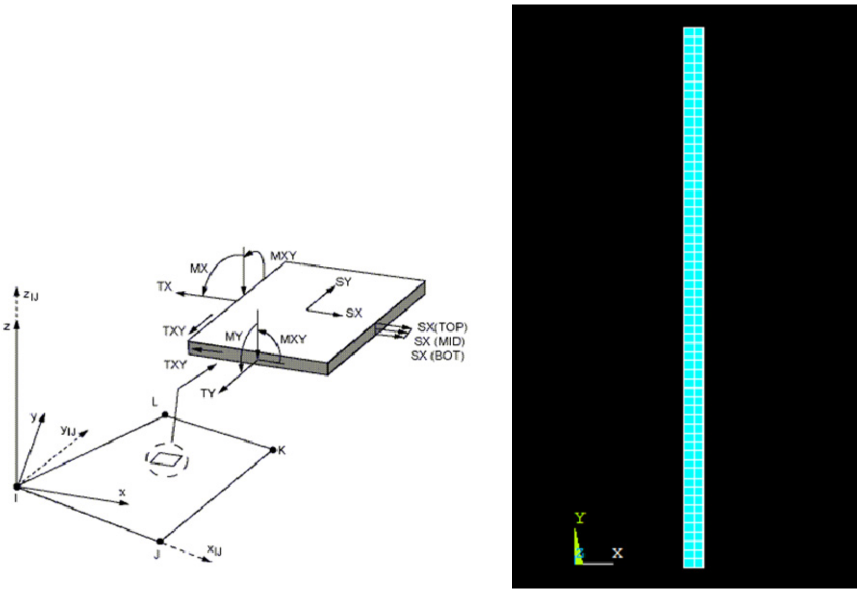

(a) (b)

Figure 3: (a) Detail of SHELL63 element from ANSYS® used to mesh plate strips. (b) Plate Strip with $L_x = 1/30\ m$, $L_y = 1\ m$, $h = 0.001\ m$, meshed with 60 elements in the y direction and 2 elements in the x direction.

The stiffness and mass matrices for the plate model including all DOFs are extracted from the FE model and the dynamic stiffness matrix built for discrete frequencies. Then, in order to obtain the dispersion curve for an infinite plate simply-supported along the x direction, rows and columns corresponding to transverse displacement and rotation about the y-direction along these edges are suppressed. Based on this new dynamic matrix, the alternative eigenvalue problem proposed in section 2.3 is solved and the dispersion curves, obtained, see Figure 4. In Figure 5, only those modes predicted by analytical solution of a plate simply-supported along two edges are plotted against the ones theoretically predicted. It is clear that those wavenumbers are very well predicted numerically.

The forced response of a plate with $(1\,m \times 1\,m)$ simply-supported at all edges and subjected to a harmonic excitation $(100\,N)$ in the transverse direction at $(x = 0.5\,m,\ y = 0.5\,m)$ is obtained by WSFEM using the procedure that has been discussed in section 3.2. In this analysis, two elements with $0.5\,m$ of length each were used, and the numerical dynamic matrices for such elements were assembled to build the global dynamic matrix for the whole plate. Then, the forced response in the frequency range $1-200\,Hz$ was calculated by inversion of the global matrix subjected to the appropriated boundary conditions. In Figure 6(a), a scheme of the analysed plate is shown and in Figure 6(b) the forced response obtained by WSFEM, with all modes included, evaluated at the excited node is compared to responses obtained analytically (SEM) and numerically by FE analysis.

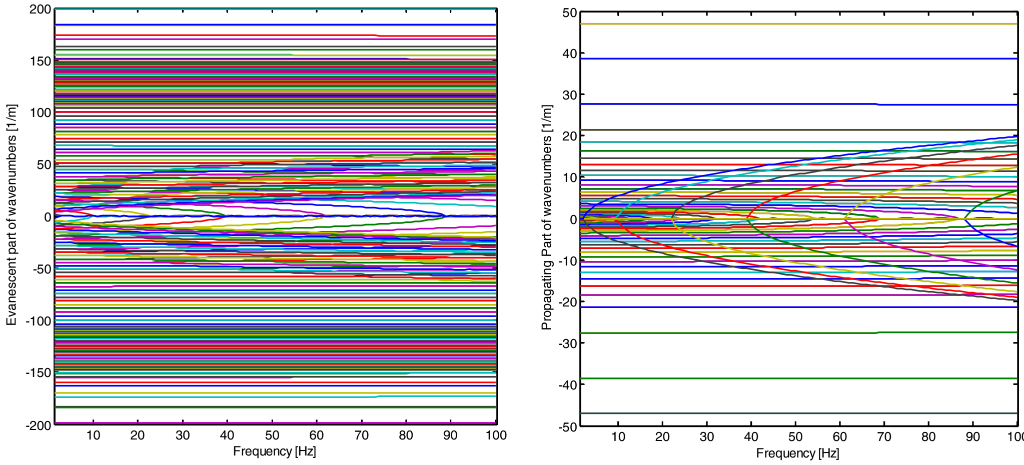

(a) (b)

Figure 4: Dispersion Curve of a steel plate with 1 m of width numerically obtained: (a) evanescent part (real) of wavenumbers within $(-200, 200)\ m^{-1}$ are plotted, (b) propagating (imaginary) part of wavenumbers within $(-50, 50)\ m^{-1}$ are plotted.

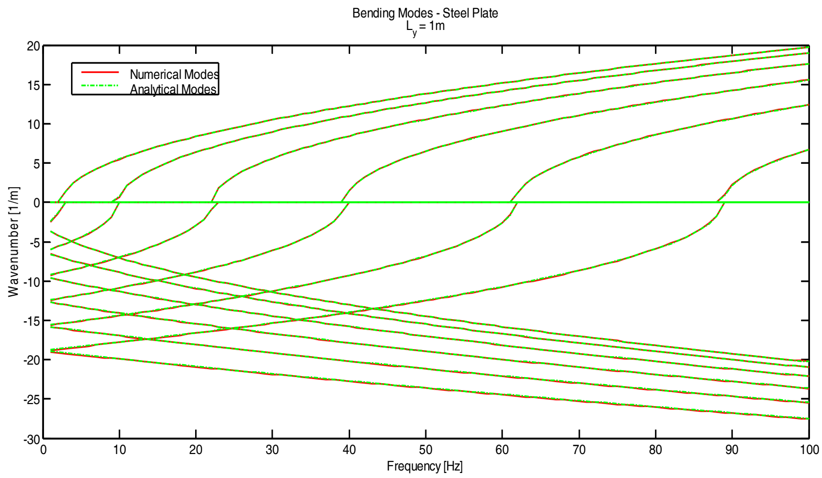

Figure 5: Dispersion curve including only bending modes of a steel plate with 1 m of width. Numerical and analytical solutions are plotted. In this plot, the following convention is adopted: positive values correspond to the real part of wavenumbers and negative values to the imaginary part of wavenumbers.

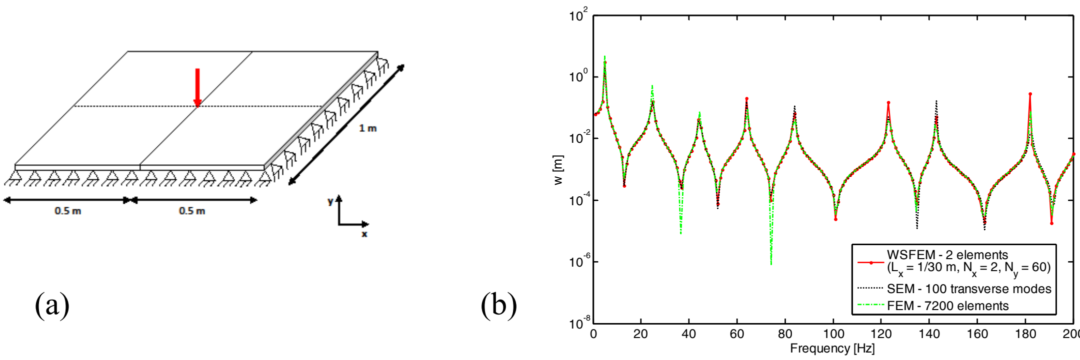

(a) (b)

Figure 6: (a) Scheme of the steel plate analysed, (b) forced response of the plate measured at the excited node.

From Figure 6(b), a good agreement between the analytical (SEM) and numerical (FEM and WSFEM) results is noticed within the frequency range considered. This validates the proposed approach for the simply-supported case.

4.2 Analysis of a free plate

In the previous section, the steel plate was analysed when simply supported at all edges. Now, the validity of WSFEM with arbitrary boundary conditions is verified, for instance, when free edges. Analysis in higher frequencies is also performed as an attempt to validate the numerical method when the number of modes increases. Since SEM does not provide analytical solutions for the free boundary condition, the numerical results by WSFEM are compared only to FE analysis results.

At low frequencies, in the $1-200\,Hz$ range, the same plate strip of the previous section, $L_x = 1/30\,m$, $L_y = 1\,m$, $h = 0.001\,m$, $N_x = 2$ and $N_y = 60$, was used to obtain the numerical results. This time, boundary conditions are not applied to the dynamic stiffness matrix for the slice built from mass and stiffness matrices extracted from FE model. The dispersion curve obtained in the free condition after solving the alternative eigenvalue problem is shown in Figure 7.

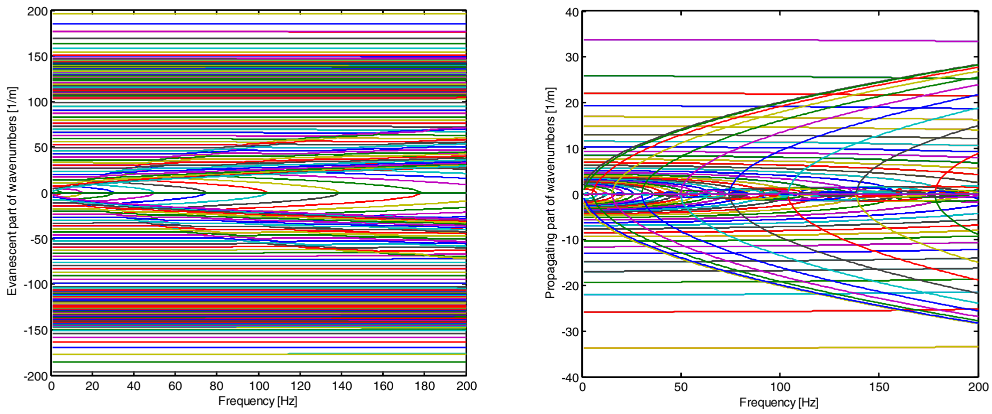

(a) (b)

Figure 7: Dispersion Curve of a steel plate with 1 m of width numerically obtained: (a) evanescent part of wavenumbers within $(-200, 200)\,m^{-1}$ are plotted, (b) propagating part of wavenumbers within $(-40, 40)\,m^{-1}$ are plotted.

Then, the WSFEM is applied to obtain the forced response of the structure in free condition when subjected to a harmonic load in the transverse direction (z) at $(x = 0.5\,m, y = 0.5\,m)$. Only two elements are used in this numerical solution and all modes within this frequency range are included. The transverse displacement response at the point of excitation is obtained and compared to FE analysis of the plate meshed with 3600 elements, see Figure 8. The result shows that the methodology used is suitable for wave propagation analysis of free plates.

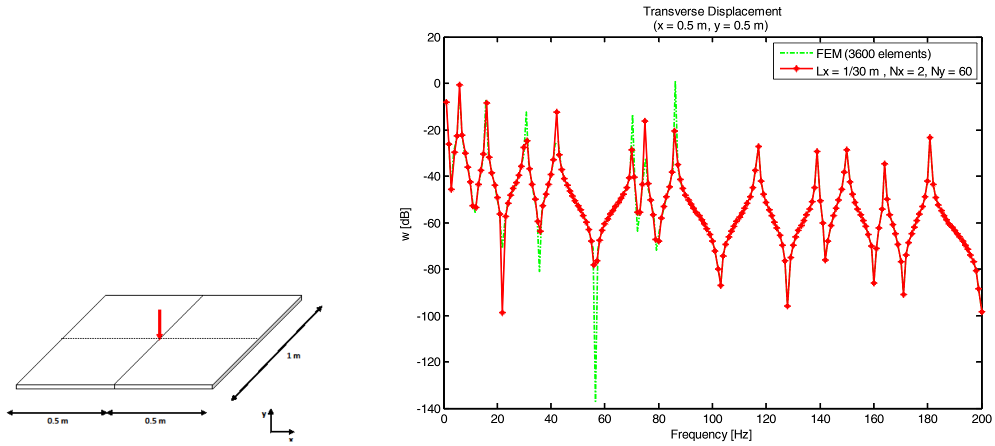

(a) (b)

Figure 8: (a) Scheme of the steel plate analysed. (b) Forced response of the plate measured at the excited node.

Now, the proposed approach will be validated for higher frequency ranges. At high frequencies, in the $950-1050\,Hz$ range, the steel plate is also analysed. In this frequency range, a refined mesh of the plate strip is required in order to obtain accurate results. For this purpose, a plate strip with $L_x = 1/43\,m$, $L_y = 1\,m$, $h = 0.001\,m$, $N_x = 2$ and $N_y = 86$ was modelled using SHELL63 finite elements in ANSYS®. The dispersion curve in free condition for this structure slice is shown in Figure 9. Comparing this dispersion curve with the one plotted in Figure 7, a higher wave modal density is observed for high evanescent wavenumbers and also propagating wavenumbers.

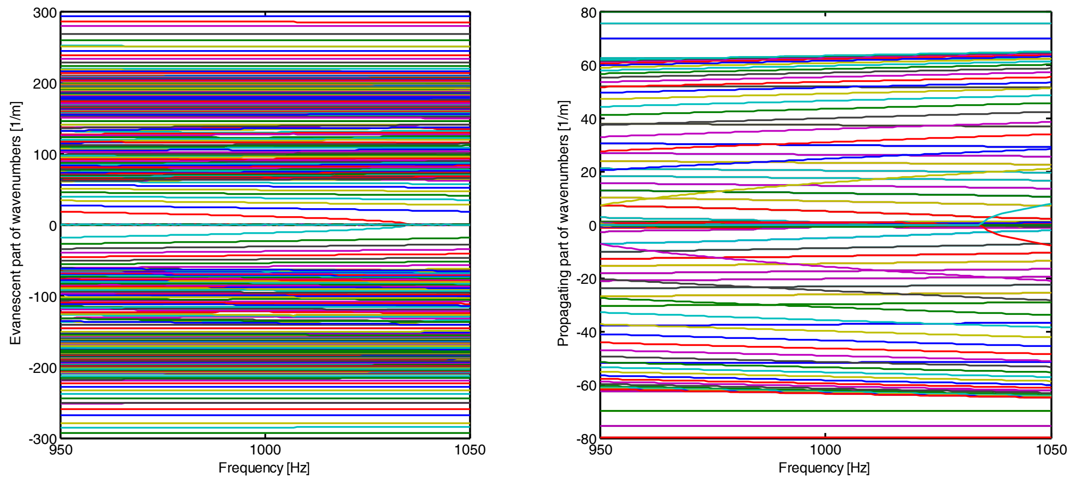

(a) (b)

Figure 9: Dispersion curve of a steel plate with 1 m of width numerically obtained: (a) evanescent part of wavenumbers within $(-300, 300)\,m^{-1}$ are plotted, (b) propagating part of wavenumbers within $(-80, 80)\,m^{-1}$ are plotted.

The forced response of the free plate with $(1\,m \times 1\,m)$, harmonically excited in the $950 - 1050\,Hz$ range at $(x = 0.5\,m,\, y = 0.5\,m)$, is also obtained by the WSFEM. The result is shown in Figure 10 plotted against the one obtained using conventional FE analysis. We see that both results are superposed, except at one frequency line. Except for the numerical divergence seen at this frequency around 1000 Hz, Figure 10 confirms the potential of WSFEM for wave propagation analysis from mid to high frequency ranges, where refined meshes are required and analytical solutions are not available.

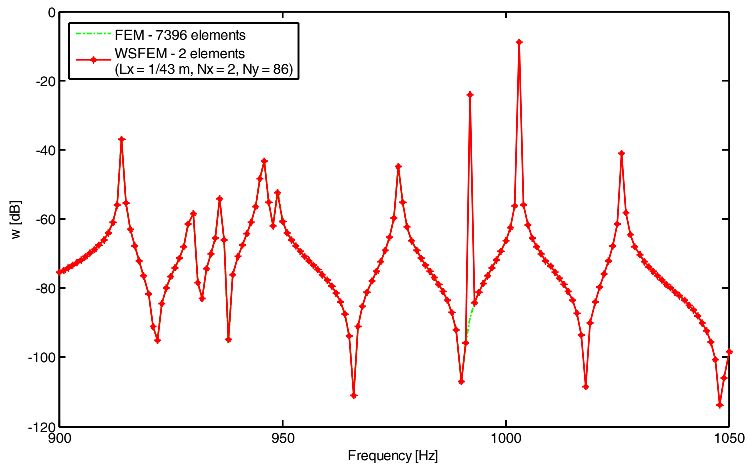

Figure 10: Forced response of a steel plate in free boundary condition measured at the excited node.

5 Conclusions

This paper has extensively described the mathematical formulation necessary for the application of the wave spectral finite element method to general, and particularly to two-dimensional structures. In this work, the thin plate in bending was the application investigated under different boundary conditions: simply supported at all edges and free at all edges. The type of problem treated has allowed the validation of the proposed approach when a large number of wave modes are included in the formulation, thus, confirming the potential of such approach in predicting higher order behaviour. It was also possible to verify that regardless of the frequency range considered or the wave modal density, the WSFEM seems to be a reliable method for studying wave propagation problems. When the computational cost is considered, the WSFEM is shown to be advantageous when compared with the conventional FEM because mesh refinement is only required in the modelling of the structure slice. When the numerical dynamic stiffness matrix for the whole structure is recovered, mesh refinement is no longer necessary as the displacement and force fields are written in the frequency domain.

References

[1] S. B. Dong and R. B. Nelson, "On Natural Vibrations and Waves in Laminated Orthotropic Plates", Journal of Applied Mechanics, 39 (3), 739-745, 1972.

[2] D. Thompson, "Wheel-rail Noise Generation, Part III: Rail Vibration", *Journal of Sound and Vibration*, 161, 421 – 446, 1993.

[3] L. Gavric, "Finite Element Computation of Dispersion Properties of Thin-Walled Waveguides", Journal of Sound and Vibration, 173, 113 - 124, 1994.

[4] D.J. Mead, "A General Theory of Harmonic Wave Propagation in Linear Periodic Systems with Multiple Coupling", Journal of Sound and Vibration 27(2), 235–260, 1973.

[5] P. Loveday, "Simulation of piezoelectric excitation of guided waves using waveguide finite elements", Ultrasonics, Ferroelectrics and Frequency Control, IEEE Transactions on, 55, 2038-2045, 2008.

[6] I. Bartoli, A. Marzani, F.L. di Scalea, and E. Viola, "Modeling wave propagation in damped waveguides of arbitrary cross-section", Journal of Sound and Vibration, 295, 685-707, 2006.

[7] T. Hayashi, W. Song and J.L. Rose, "Guided wave dispersion curves for a bar with an arbitrary cross-section, a rod and rail example", Ultrasonics, 41, 175–183, 2003.

[8] V. Damljanovic, R. L. Weaver, "Forced response of a cylindrical waveguide with simulation of the wavenumber extraction problem", J. Acoust. Soc. Am., 115, 1582–1591, 2004.

[9] S. Finnveden, Exact spectral finite element analysis of stationary vibrations in a railway car structure, Acta Acustica, 2, 433–449, 1994.

[10] D. Duhamel, B.R. Mace, M.J. Brennan, "Finite element analysis of the vibrations of waveguides and periodic structures", Journal of Sound and Vibration, 294, 2006.

[11] B.R. Mace, D. Duhamel, M.J. Brennan, L. Hinke, "Finite element prediction of wave motion in structural waveguides", J. Acoust. Soc. Am., 117(5), 2835-2843, 2005.

[12] J.-M. Mencik, "On the low- and mid-frequency forced response of elastic structures using wave finite elements with one-dimensional propagation", Computers and Structures, 88, pp 674-689, 2010.

[13] J. R. F. Arruda, K.M. Ahmida, M.N. Ichchou, J.M. Mencik, "Investigating the relations between the wave finite element and spectral element methods using simple waveguides", 19th International Congress of Mechanical Engineering-COBEM, 2007.

[14] J.R.F. Arruda, R.F. Nascimento, "Building spectral element dynamic matrices using finite element models of waveguide slices," Proceeding of the NOVEM 2009, Noise and Vibration: Emerging Methods, Oxford, 2009.

[15] W. Yao, W. Zhong, C.W. Lim, "Symplectic Elasticity", World Scientific Publishing, 2009.

[16] J.F. Doyle, "Wave Propagation in Structures", 2nd. Edition, New York: Springer, 1997.

[17] Y. Waki, “On the application of finite element analysis to wave motion in one-dimensional waveguides”, PhD Thesis, University of Southampton, Institute of Sound and Vibration Research, 2007.